ELSEVIER

Advances in Water Resources 24 (2001) 1211–1227

Advances in Water Resources

www.elsevier.com/locate/advwatres

Evaluation of hydrologic equilibrium in a mountainous watershed: incorporating forest canopy spatial adjustment to soil biogeochemical processes

D. Scott Mackay *

Department of Forest Ecology and Management, Institute for Environmental Studies, University of Wisconsin-Madison, 1630 Linden Dr., Madison, WI 53706, USA

Received 15 June 2000; received in revised form 11 January 2001; accepted 2 February 2001

Abstract

Hydrologic equilibrium theory has been used to describe both short-term regulation of gas exchange and long-term adjustment of forest canopy density. However, by focusing on water and atmospheric conditions alone a hydrologic equilibrium may impose an oversimplification of the growth of forests adjusted to hydrology. In this study nitrogen is incorporated as a third regulation of catchment level forest dynamics and gas exchange. This was examined with an integrated distributed hydrology and forest growth model in a central Sierra Nevada watershed covered primarily by old-growth coniferous forest. Water and atmospheric conditions reasonably reproduced daily latent heat flux, and predicted the expected catenary trend of leaf area index (LAI). However, it was not until the model was provided a spatially detailed description of initial soil carbon and nitrogen pools that spatial patterns of LAI were generated. This latter problem was attributed to a lack of soil history or memory in the initialization of the simulations. Finally, by reducing stomatal sensitivity to vapor pressure deficit (VPD) the canopy density increased when water and nitrogen limitations were not present. The results support a three-control hydrologic equilibrium in the Sierra Nevada watershed. This has implications for modeling catchment level soil–vegetation–atmospheric interactions over interannual, decade, and century time-scales.

Keywords: Hydrologic equilibrium; Leaf area index; Transpiration; Photosynthesis; Nitrogen cycling; Carbon allocation; Distributed hydrology simulation; Mountainous catchment; Forest ecosystem

1. Introduction

An understanding of vegetation–soil–topography in relation to climate is essential for predicting both the short- and long-term hydrologic responses of catchments. Land use, atmospheric CO_2 increases, and other aspects of human impact on global ecosystems affect ecosystems at all spatial scales, including landscape and watershed level, and over long time periods. Attempts to formulate an integrative understanding of vegetation, soils, and hydrologic relations at regional scales, including Eagleson's [7] ecological optimality, have emphasized the existence of equilibrium conditions between water demand and supply. This paper builds on this concept of an equilibrium adjustment of natural forested ecosystems to hydrologic flow paths and climatic controls, by incorporating a rate-limitation controlled by soil biogeochemical cycling. The focus is on canopy density at the catchment scale, which is a key determinant of evapotranspiration and carbon assimilation rates. It is proposed that canopy density in old-growth, conifer covered mountainous catchments can be explained by (1) available water, (2) atmospheric vapor pressure deficit (VPD), and (3) rates of nitrogen mineralization. The first two elements of this proposition are reasonably well accepted and are incorporated into many ecosystem-oriented catchment models [2,45,49]. Available water is a function of soil texture and topography-controlled recharge. It ultimately influences canopy density through water limitation, which lowers stomatal conductance rates [16], and hence carbon assimilation rates. Water limitations are also partly used to explain the relative allocation of carbon to foliage versus roots; field evidence suggests that plants on drier

* Tel.: +1-608-262-1669; fax: +1-608-262-9922.
E-mail address: dsmackay@facstaff.wisc.edu (D.S. Mackay).

0309-1708/01/$ - see front matter
PII: S0309-1708(01)00040-9

sites tend to allocate proportionally more resources to their roots [9,19].

Atmospheric vapor pressure also reduces stomatal conductance through a physiological response to high evaporative demand [17,30] (Fig. 1). These canopy density adjustments to climate and soil were summarized in Eagleson's ecological optimality theory [7] and demonstrated in natural ecosystems [31]. The latter authors used the term *hydrologic equilibrium*, which is adopted here because it neither implies internal plant controls on its environment [5,48] nor plant responses to external environmental controls [28]. The specific physiological control on stomatal guard cell response to VPD remains controversial, but it is generally accepted that when plants are at the brink of becoming water-limited high VPD promotes stomatal closure [21]. For hydrologic purposes it may be sufficient that as VPD increases there is a critical point at which transpiration ceases to increase and may start to decline. This may be attributed to a balance point in which stomatal closure is sufficiently large to offset evaporative demand. With reduced gas exchange rates carbon assimilation is in turn reduced by stomatal closure (Fig. 2).

Numerous attempts at formulating a general theory to describe the soil–vegetation–atmospheric continuum have postulated the existence of such a hydrologic equilibrium. Under an equilibrium hypothesis vegetation adjusts to maximize its growth while minimizing water stress. Such theories have been utilized to develop simple models of terrestrial vegetation distribution at local [13,31], regional [1], and global scales [50]. Although general trends in canopy density can be explained by hydrologic equilibrium theory, it is suggested here that this oversimplifies most natural systems. Almost all natural forested ecosystems are nutrient (or nitrogen)-limited. The nitrogen (N)-limitation occurs because rates of nitrogen mineralization ultimately do not keep pace with potential carbon fixation rates implied by hydrologic equilibrium. The

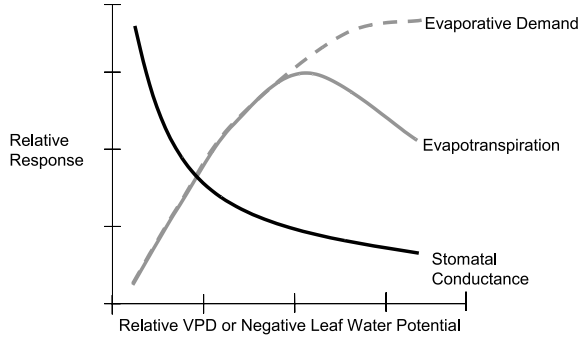

Fig. 1. Stomatal conductance tends to decline as vapor pressure deficit (VPD) increases. Simultaneously, evaporative demand increases to some limiting factor such as degree of canopy–atmospheric coupling and radiation. Evapotranspiration can decline under some conditions of relatively low soil water and high VPD.

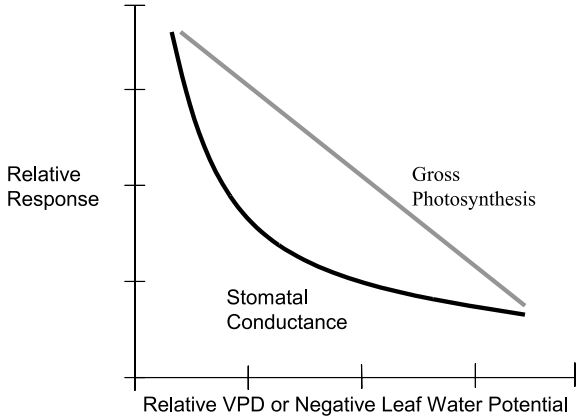

Fig. 2. Gross photosynthesis declines roughly linearly with VPD as a result of reduced stomatal aperture opening.

rate at which N is made available for vegetation uptake depends largely on turnover rates, which are proportional to above-ground biomass, on rates of microbial activity, which depend on soil temperature and moisture conditions, and on N losses, which tend to be the greatest during times of vegetation dormancy. In addition, there is generally a long lag time (10^1–10^2 years) between biomass turnover and nutrient release in the soil. These factors contribute to a capacitance in the soil or a soil "memory effect." Two observations can be made about this: (1) in aggrading forests the canopy density and soil carbon and nitrogen content may be unrelated, but (2) in old-growth or otherwise steady-state forests there should be a direct correlation between canopy density and soil carbon and nitrogen content [40]. The purpose of this paper is to evaluate this extended hydrologic equilibrium by recognizing that almost all natural forest ecosystems are N-limited. We hypothesize a three-component equilibrium consisting of water limitation,

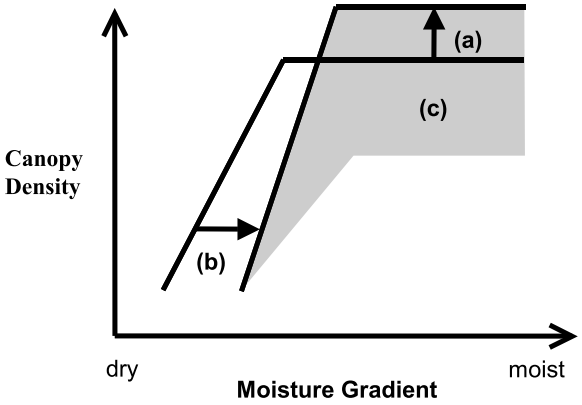

Fig. 3. Proposed modified hydrologic equilibrium, which includes: (a) a VPD-controlled maximum or potential canopy density; (b) a soil moisture stress factor that may incorporate recharge and soil texture; and (c) a region below the line of potential canopy density, which reflects nitrogen limitation on canopy growth.

climate (or VPD) limitation, and nitrogen availability limitation (Fig. 3).

In the following section we describe a catchment that is well suited for an analysis of hydrologic equilibrium. This is followed by a description of the catchment model used, the approach used to evaluate the three-component equilibrium theory, results and discussion, and then some conclusions.

2. Study site

The catchment for this study is the Onion Creek Experimental Forest (Fig. 4), a 10 km^2 watershed located along the crest of the Central Sierra Nevada of California. Relief within the watershed is about 1000 m with the highest elevation at about 2600 m above mean sea level. Vegetation cover is predominantly undisturbed old-growth mixed conifers with dominant tree species of White Fir (*Abies concolor*), Red Fir (*Abies magnifica*), Sugar Pine (*Pinus lambertiana*), Jeffrey Pine (*Pinus jeffreyi*), Lodgepole Pine (*Pinus contorta*), and Incense Cedar (*Calocedrus decurrens*). Cedar species generally occupy lower elevations and fir species occur at higher elevations. Annual precipitation here is on average 1300 mm, of which 90% falls as snow between October 1 and March 31. Soils are generally poorly developed loamy sands, underlain by rhyolitic ash and thick latite deposits with relatively high permeability and large storage capacity [25]. The nearby Central Sierra Snow Lab (at 2100 m a.m.s.l.) regularly shows maximum snow water equivalents of a meter or more, although the predominantly south-facing slopes of Onion Creek have much lower snow depths. Snow melt is the primary source of soil water, much of which is stored in the basin for several weeks following the end of snow melt (by mid- to late-May). Research on ground water flow in Onion Creek has shown a high storage capacity in the soils and underlying parent material and long lags in the baseflow recession [26]. The stored water represents a potentially large source of available water needed to sustain the forested vegetation through extremely dry summer months.

3. Model description

3.1. Primary controls on canopy gas exchange

The catchment model used here is a dynamic canopy version of the Regional Hydro-Ecological Simulation System (RHESSys) [27]. The model combines forest ecosystem process components adapted from FOREST-BGC [36,37], a catchment-based hydrological model using TOPMODEL [4], and a climate simulation system, MT-CLIM [39]. Simulation over large, heterogeneous watersheds is facilitated by dividing the landscape into a series of facets or hillslope partitions based on geomorphometric principles. Hillslope partitions capture most of the variance in incident short-wave radiation, which means that partitions can be simulated in parallel. Catenary variations of topography, soils and

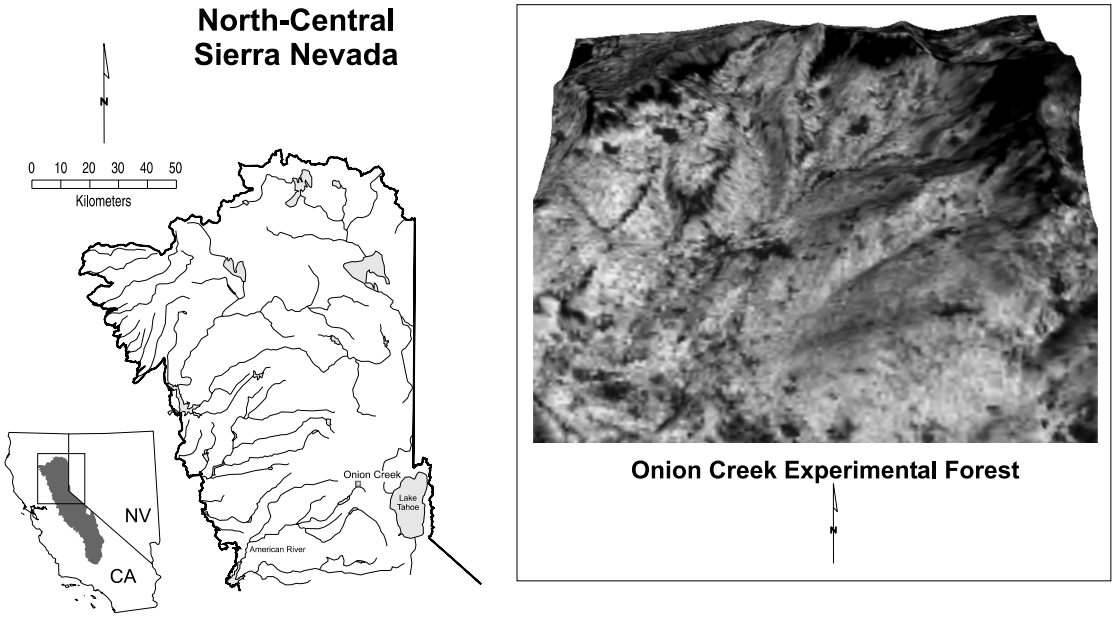

Fig. 4. Location of our study site within the Sierra Nevada. The image shows a perspective rendering derived from a 30 m DEM with LAI draped over the surface. In this view looking northward the sun is located in the southeast in order to highlight southeast-facing and southwest-facing slopes in the watershed.

vegetation within each hillslope are then incorporated as distributional information within hillslope partitions (Fig. 5). The distributional information accounts for the variability of lateral subsurface flow, ET, soil drainage, snowmelt, and canopy photosynthesis [2].

Within-hillslope variability in air temperatures and snow melt rates are captured with elevation zones. Within-hillslope variability in flow convergence–divergence, soil hydraulic properties, and land cover characteristics are represented using distributional information derived using a topography–soils index (TSI) [3,4,42]. Soil water retention and drainage, snow melt, and ET processes are then simulated at the resolution of the within-hillslope distributional level, and are thus influenced by hillslope-level radiation and elevation-specific air temperatures.

Drainage from the unsaturated soil zone is modeled using [44]. Water lost from the unsaturated zone through transpiration may be replenished by capillary rise, which is implemented as a steady-state solution of the Richards Equation [10]. Evaporation directly from soils is not implemented. Instead, simulated forest soil is covered with a leaf litter layer and evaporation from this layer is based on relative humidity. For Onion Creek litter evaporation is negligible during the period in which we conducted our analysis. This design is optimal

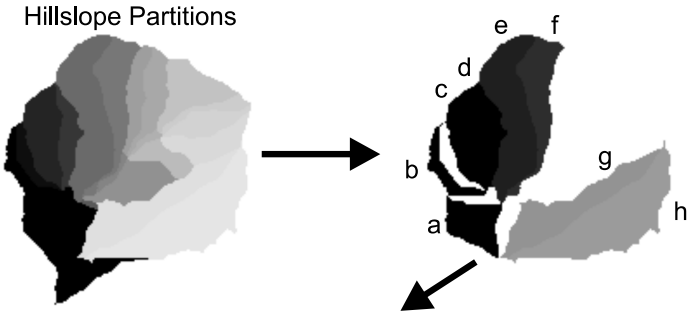

Partition Mean Parameters

Label	Aspect	Elevation	Slope	Area	Lambda	# Elevation Zones
	(deg)	(m)	(deg)	(pixels)	(m)	
a	111	1896	12.8	719	8.11	10
b	92	2041	10.2	334	7.47	11
c	133	2109	15.5	919	7.12	15
d	220	2075	13.7	485	7.08	15
e	120	2061	16.8	1769	7.13	18
f	239	2092	18.6	1024	6.99	19
g	204	1993	9.9	1368	7.64	21
h	277	2112	12.9	2172	7.64	22

Portion of Distributional Information

Elevation	TSI	Area	LAI	Ksat	RL	b	theta_r	psi_f
(m)	(m)	(pixels)	(m2/m2)	(cm/day)	(cm)			(cm)
1812								
	7.57	17	8.46	304.0	169.1	0.654	0.024	17.2
	8.52	49	9.25	254.2	184.9	0.583	0.032	19.1
	9.41	24	7.30	244.0	146.0	0.569	0.033	19.5
	10.56	2	8.50	231.1	170.0	0.550	0.035	20.0
	11.82	1	5.00	334.3	100.0	0.698	0.020	16.0
	12.61	1	14.75	334.3	295.0	0.698	0.020	16.0
	13.78	2	7.88	282.7	157.5	0.624	0.027	18.0
	14.74	2	8.50	475.7	170.0	0.698	0.020	16.0
	15.46	5	7.25	251.7	145.0	0.580	0.032	19.2
	16.44	13	7.94	286.7	158.8	0.630	0.027	17.8
	17.47	3	6.50	231.1	130.0	0.550	0.035	20.0

Fig. 5. The simulation model divides a watershed into a series of hillslope partitions, which are hydrologically well defined and allow for the use of partition average solar radiation. Of the 26 partitions we selected 8 that were deemed representative of the watershed. Their mean parameters are shown. Lambda is the partition mean TSI used in TOPMODEL. Each partition is also divided into a series of elevation zones and within each zone a table of distributional information is defined using patches derived from TSI. All cells aggregated into a given TSI patch are hydrologically similar. Other variables, including LAI, saturated hydraulic conductivity (K_{sat}), rooting length (R_L), soil pore-size distribution index (b), residual soil water content (theta_r), height of the capillary fringe (psi_f) are averaged within each of the patches. For all 26 hillslope partitions there are about 1600 TSI patches, compared to the approximate 11,000 30 m pixels within the watershed.

under a reasonably closed forest canopy in which very little radiation penetrates to ground level, or in open areas when near surface soil moisture is very low and precipitation is infrequent. In general, water in the rooting zone is related to the position of the water table when soils are recharged and becomes more related to cumulative ET as soil water is drawn down.

Water, carbon, and nitrogen fluxes and stores are shown in Fig. 6. The model distinguishes between wet and dry canopies. Evapotranspiration from dry canopies is calculated using the Penman–Monteith [29] combination equation,

$$\mathrm{LE} = \frac{\Delta R_c + \rho_a c_p D / r_a}{\Delta + \gamma(1 + r_c/r_a)}, \quad (1)$$

where LE is the latent heat flux (m s^{-1}), R_c is the net canopy absorbed radiation (W m^{-2}), Δ is the slope of the saturation vapor pressure–temperature curve (mb °C^{-1}), $\rho_a c_p$ (J m^{-3} °C^{-1} is the specific heat density of air, D (mb) is the VPD, r_a (s m^{-1}) is the bulk aerodynamic resistance for latent heat transfer between the vegetation canopy and its surrounding atmosphere, γ (mb °C^{-1}) is the psychrometric constant, and r_c (s m^{-1}) is the canopy total stomatal resistance. Canopy resistance is the reciprocal of canopy conductance, which is calculated as the product of LAI and average leaf level stomatal conductance. We assume that leaf level stomatal conductance is reduced from maximum rates as a function of ambient VPD, soil moisture, light levels, and soil temperature factors [23]. Bulk canopy aerodynamic resistance is set at 5.0 s m^{-1} for well ventilated, closed conifer canopies, but can be increased as the canopy opens up to bare ground (100 s m^{-1}) [46]. In the absence of wind data and detailed canopy height characteristics, r_a is difficult to describe spatially. Most of our study site has a dense canopy, and so the spatial variability of r_a should not be too critical to our analysis.

Gross photosynthesis is given by

$$\mathrm{GSPN} = \frac{\Delta \mathrm{CO}_2 c g_c g_m}{g_c + g_m}, \quad (2)$$

where ΔCO_2 is the gradient partial pressure of CO_2 between intercellular and ambient atmosphere, c is a

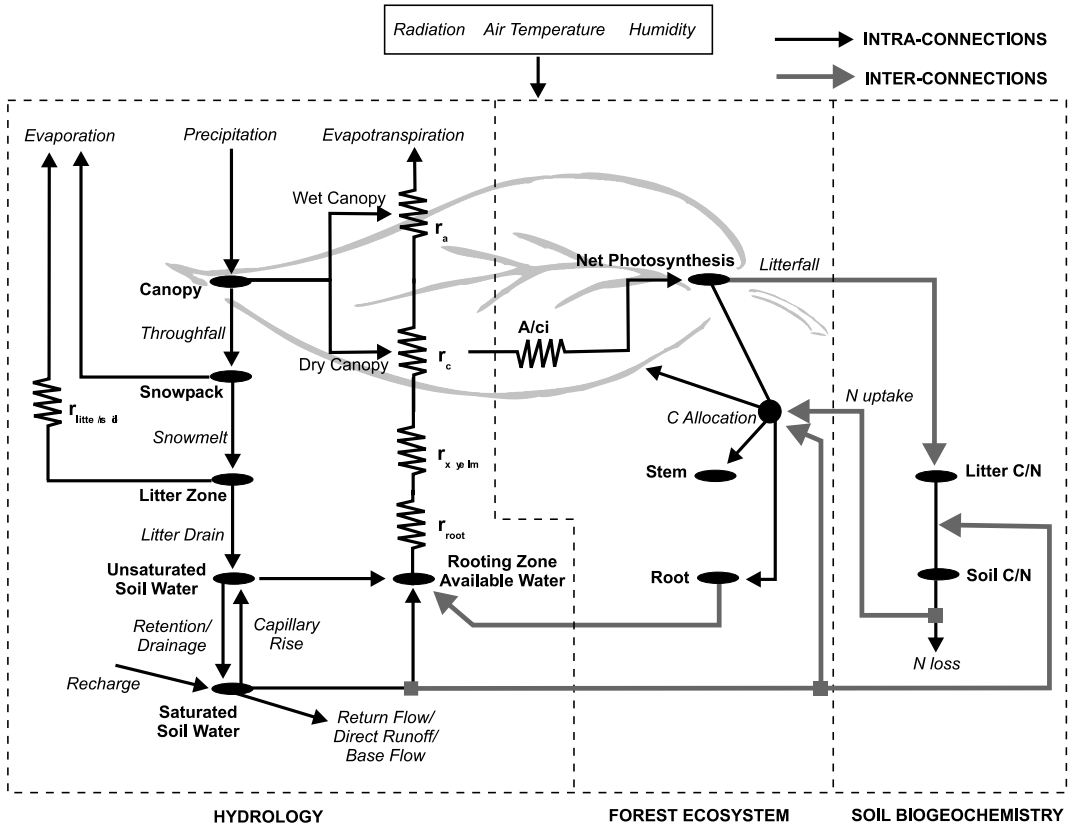

Fig. 6. Major hydrologic, forest ecosystem, and soil biogeochemistry components of the simulation model used in this study. The canopy is represented as a big leaf for each landscape patch. A dry canopy follows the Penman–Monteith (P–M) combination equation, while a wet canopy uses a modified P–M with bulk canopy resistance, r_c, set to infinity. Daily photosynthesis depends on stomatal conductance, mesophyll conductance (A/ci), and leaf nitrogen content. A rooting zone is superimposed on the two layer soil structure (saturated and unsaturated zones) and is used to determine plant available water. During dry summer months the only source of ET is from the vegetation canopy, as the litter zone quickly dries and there is no soil evaporation in the model. Carbon allocation is driven by water and nitrogen limitations. Nitrogen availability is maintained with a two-layer soil decomposition model.

constant correction factor for CO_2 versus H_2O gas exchange, g_c is average leaf-level stomatal conductance, and g_m is the rate of assimilation per unit of intercellular CO_2.

3.2. Equilibrium model of canopy density adjustment

An explicit canopy model is coupled with the distributed hydrology [27]. The model performs annual carbon (C) allocation [37], and it has nonlinear, daily models of nitrogen mineralization and loss controlled by soil moisture, soil temperature, and C/N ratios. A nitrogen budget is maintained to support canopy photosynthesis and the allocation of carbon to leaves and roots. Net annual assimilated C is allocated to foliar, stem, and root compartments by calculating a leaf-root ratio:

$$R_{L/R} = (I_\theta + I_N)/4, \tag{3}$$

where I_θ is a soil moisture index computed as the average growing season fraction of soil moisture in the rooting zone, and I_N is a dimensionless parameter of nitrogen availability computed as

$$I_N = \frac{N_A}{\Lambda^* N_{Lmax}} N_{L/R}. \tag{4}$$

$N_{L/R}$ is a leaf-root nitrogen allocation parameter, Λ^* is potential leaf carbon (kg C ha^{-1}), and N_{Lmax} (kg N kgC^{-1}) is maximum leaf nitrogen concentration, which is also set as a site-specific parameter, and N_A (kg N ha^{-1}) is available nitrogen. Actual leaf carbon allocation is calculated as the minimum of available photosynthate and the amount of carbon that can be supported by the given N_A. Allocation to roots is determined from allocated leaf carbon divided by $R_{L/R}$. Greater allocation to the roots satisfies a need for a larger root structure to obtain limited nitrogen or water resources [19]. A separate logic, described below, is used to extend roots downward in response to water limitation. After carbon has been allocated to foliar and root compartments any remaining carbon is added as stem growth increment.

Plant available water is determined by superimposing R_L on the two-layer soil model (see Fig. 2). R_L is difficult to directly observe in individual stands and intractable over large areas in variable topography. Most distributed hydrology models prescribe a uniform R_L based on little or no direct measurement, and with more regard for expected soil depths than for the physiological processes governing vegetation hydraulic regulation. Carbon allocation logic has previously been used [45] to control growth rates of rooting depths or lengths, R_L. A problem with this approach is that an increased allocation of carbon to roots in response to N limitation would not likely promote greater rooting depth, since N concentrations are generally low at greater depths. However, it is reasonable that water limitation would promote root downward extension.

For a given site moisture status a large canopy with a high LAI should need a greater R_L. Considered just in terms of water balance it is not unreasonable that for a given climate and hydrologic regime a high LAI must be supported by greater R_L than a low LAI. Using a simple dimensional analysis the spatial distribution of potential R_L can be described with the following relation:

$$R_L = \frac{R'\mathrm{LAI}}{(\mathrm{TSI}/\lambda)}, \tag{5}$$

where R' is a parameter describing rooting length per unit LAI (m) for an average water availability site, and is a hillslope partition mean TSI. Potential R_L is scaled upward in proportion to canopy water demand as represented by LAI and scaled downward in proportion to relative profile water availability. For example, a very dry site supporting a large LAI would have a large potential R_L, a wet site supporting a large LAI can have a smaller R_L, and a site with a low LAI need only have a small potential R_L. These relations are common in forested watersheds in which wetter sites near streams tend to have shallower rooted trees than drier sites. In order to use Eq. (5) it must be plausible for the vegetation to take some form of equilibrium with the climate-hydrology regime, which is reasonable for an old-growth forest not subject to recent disturbance. Given the relatively rapid response of tree root systems to changing site conditions [22] this assumption may be reasonable for a wide range of forest ecosystem types. However, it should be noted that Eq. (5) describes a potential rooting depth that is independent of carbon allocation. Because there is a carbon cost associated with growing roots the actual R_L is increased only when there is a positive change in root carbon allocation. The actual increase in R_L is then proportional to the rate of change in root carbon.

Canopy growth dynamics are maintained by cycling of carbon and nitrogen through a soil (or humus) layer, a litter layer, roots, stems, and leaves. No passive soil carbon pool is included, as this takes millennia to turnover and is unlikely to respond to short-term perturbations, such as human-induced climate change or land use [14]. An available nitrogen budget is maintained as follows:

$$\frac{dN_A}{dT} = N_{Fert} + N_{Ret} + M_{Lit} + M_{Soil} - (N_{Turn} + N_{Stem} + N_{LOSS}), \tag{6}$$

where N_{Fert} (kg N ha^{-1}) is a daily input of nitrogen deposition or fertilization, N_{Ret} (kg N ha^{-1}) is the amount of nitrogen recycled internally (or retranslocated) from the leaves prior to leaf drop. Leaf drop timing for conifers is given as a function of I_N to allow needles to

remain in the canopy longer under nutrient poor conditions. Mineralized nitrogen from litter, M_{Lit} (kg N ha^{-1}), and humus, M_{Soil} (kg N ha^{-1}), and nitrogen loss, N_{LOSS} (kg N ha^{-1}), are computed daily. Decomposition rates are determined by two rate functions, respectively, for soil temperature and soil water. The temperature rate is given by an Arrhenius function:

$$F_T = \exp\left(\frac{b(T_{\mathrm{soil}} - T_{\mathrm{ref}})}{T_{\mathrm{soil}} \cdot T_{\mathrm{ref}}}\right), \tag{7}$$

where T_{soil} (°C) and T_{ref} (°C) are, respectively, the actual soil temperature and the optimal soil temperature for decomposition, assumed here to be 35 °C. The b parameter is set to a Q_{10} of 2.36 [20]. The soil moisture rate factor is computed by a quadratic relationship [47]:

$$F_\theta = 1 - P(\theta)(\theta_{\mathrm{FC}} - \theta)^2, \tag{8}$$

where P is a function describing the shape of the quadratic relationship and yields a soil moisture decomposition rate factor between 0 and 1. Eq. (8) yields optimal decomposition rates when soils are at field capacity, and a reduction of decomposition rates as the soil approaches saturation.

Nitrogen mineralization rates follow a logic used in BIOME-BGC [38]. These rates are given, respectively, by

$$M_{\mathrm{Lit}} = N_{\mathrm{Lit}} D_{\mathrm{L}} D_{\mathrm{N/C}} (1 - \mathrm{lignin}) \tag{9}$$

and

$$M_{\mathrm{Soil}} = N_{\mathrm{S}} D_{\mathrm{S}}, \tag{10}$$

where $D_{\mathrm{N/C}}$ is a parameter describing the relative rate of nitrogen and carbon decomposition, N_{Lit} (kg N ha^{-1}) and $\mathrm{N_S}$ (kg N ha^{-1}) are, respectively, litter and soil nitrogen. Litter decomposition rate, D_{L}, and humus layer decomposition rate, D_{S}, are proportional to $(F_T \times \mathrm{F}_\theta)$ and are reduced linearly as the C:N ratios of the respective soil layers increase. A recent study in the Sierra Nevada [12] showed that pine ecosystems were insensitive to small changes in temperature. Also, recent findings [11] support the need for multiplicative controls on microbial rates, since these tend to acclimate at different temperatures.

Nitrogen loss is computed using a nonlinear function of the total available N and soil moisture conditions. The rate of N loss is given by

$$N_{\mathrm{LOSS}} = \exp\left(\frac{(N_{\mathrm{A}} - N_{\mathrm{P}})K(\theta)}{N_{\mathrm{RET}}}\right), \tag{11}$$

where N_{P} is an estimate of nitrogen required for plant uptake, $K(\theta)$ is hydraulic conductivity as a function of moisture content [44], and N_{RET} is a mobile nitrogen retention time parameter.

4. Methodology

4.1. General approach

Recall that we hypothesized the existence of three primary factors limiting canopy density: (1) water balance, (2) nutrient dynamics, and (3) VPD-controlled stomatal gas exchange. The three components of this equilibrium theory were examined in terms of (1) the spatial distribution of gas exchange along catenary sequences at sub-hillslope levels, (2) canopy density (or leaf area index (LAI)) as predicted using different strategies for initializing the soil biogeochemistry, and (3) integrated system responses to different stomatal sensitivities to VPD. These are described in the following sections. Spatial distribution of gas exchange was evaluated by comparing remotely sensed energy balance and modeled energy balance, along with water use efficiency (WUE) along sub-hillslope gradients. A catchment average time-series of Bowen Ratio, predawn leaf water potential, and WUE was also examined.

4.2. Water and energy budgets using a prescribed canopy

Total energy absorbed (R_n) by land areas or water bodies may be used to either evaporate water (LE) or heat the surface (H). The surface energy balance can be expressed as

$$\mathrm{LE} = R_n - H - G, \tag{12}$$

where G is soil heat flux. Simplified energy balance equations have been developed for use with remotely sensed imagery. They have the following form [6,15,32,41]:

$$R_n - \mathrm{LE} = B(T_{\mathrm{s12}} - T_{\mathrm{a12}})^n, \tag{13}$$

where T_{s12} and T_{a12} refer, respectively, to surface and air temperature at peak sun elevation (i.e., solar noon), and B and n are parameters. Henceforth, R_n and LE refer, respectively, to daily total canopy absorbed radiation and latent heat energy, which can be expressed in water equivalent amounts (mm). At daily time steps G is assumed to be negligible. Also, from now on we will use the terms T_{S} and T_{a} when referring to temperatures at peak sun elevation. T_{S} was derived from digital thermal data acquired with the NASA-Ames Research Center's airborne Thematic Mapper Simulator (TMS), a Daedelus scanner flown aboard a U-2 aircraft on July 2 and August 6, 1985. These data were previously corroborated with field observations made in one a subcatchment of Onion Creek [34].

4.3. Soil carbon and nitrogen initialization

One of the most difficult tasks of operating a long-term model with a soil biogeochemistry component is

the selection of initial litter and humus C and N values. This is especially difficult for distributed simulations, as it is unreasonable to expect uniform values across a catchment. Short-term distributed models typically require one to several years of spin-up time to allow for the internal adjustment and removal of state initialization effects. The adjustment period often only has to pass through a single water year in order to properly establish the soil water deficits and snowpack amounts. Simulations with a prescribed canopy have no long-term effects of initial state variable conditions on water budgets. With the introduction of a fully coupled canopy and supporting soil biogeochemical models a number of additional state variables are introduced. Some of these are involved in feedbacks that influence simulations over long periods of time. The adjustment of LAI has an immediate effect on the productivity and biomass turnover amounts over one to a few years. However, LAI should adjust quickly to environmental conditions. In addition, it is relatively straightforward to obtain reasonable initial estimates of LAI even if the model is used in a fully dynamic mode.

The same is not true for the initialization of belowground C and N pools. Full litter turnover typically requires several years and full humus layer turnover can take on the order of a century [40]. It is conceivable that initial conditions in these pools can persist within a model simulation for an extremely long spin-up period. The cost of the added model complexity is a need for an initialization period of one to several centuries. It has been shown that spatially uniform initial belowground C and N pools were adjusted over time to be spatially variable [27]. However, two key observations can be made about these adjustments: (1) It is generally not possible to initialize the modeled soil pools to reflect the long-term site history (e.g., disturbance), and (2) initially unrealistic soil carbon and nitrogen pools affect above-ground productivity and allocation that in turn affect turnover and ultimately establishes an incorrect and persistent feedback on modeled soil biogeochemistry. The first observation refers to factors such as disturbance history, long-term vegetation growth, climate variability, trends in N deposition, and other nonsteady-state controls on the soil biogeochemistry. For example, soil carbon initially drops following the removal of vegetation because of a reduction in litter turnover and an accelerated rate of decomposition with higher temperatures, moisture and nitrogen content [40]. The rate and amount of recovery of soil carbon then depends on how quickly a vegetation cover can establish on the disturbed site, the quality of litter produced by the newly established vegetation, and site factors that control soil temperature and moisture.

The second observation is that initial conditions in the soil can be expected to influence the early N uptake rates and carbon sequestration rates during simulation model initialization. Patterns of N uptake then influence early vegetation growth rates. Sites that have an overestimate of N mineralization will overestimate productivity and canopy density, and sites with underestimated available N will underestimate productivity and canopy density. Naturally, a more rapid aboveground growth will more rapidly deplete the soil N pool. This in turn reduces productivity and should adjust the canopy density and turnover rates towards some equilibrium. It seems reasonable that a sufficiently large number of simulation iterations should converge on some equilibrium relationship between aboveground and belowground carbon and nitrogen pools. However, from the first observation, above, the adjusted state variables will reflect model structure and any limited knowledge of site history. An alternative approach would be to somehow incorporate information about site history in order to initialize the litter and soil C and N pools.

To examine these ideas two approaches were taken to initialize the C and N pools. For the first approach the model was run through a 100-year period with initially spatially uniform litter and humus C and N values. Climate forcing was simplified by recycling the 1985 meteorological data from Soda Springs, CA. LAI was started at a uniform value of 1.0 and permitted to grow. This allows for a mutual adjustment of aboveground and belowground carbon pools with no a priori spatial knowledge of the system. For the second approach it was assumed that the old-growth forest in Onion Creek was in equilibrium with respect to carbon and nitrogen cycling, such that the belowground carbon pools were correlated with LAI. This assumption is justified on the grounds that a majority of the carbon that is cycled through the litter and then the humus layers is derived from leaf fall. Leaf fall is in turn proportional to the total leaf biomass. For this simulation the soil carbon pools were linearly scaled to leaf carbon estimated from the remotely sensed LAI divided by specific leaf area [38]. As with the previous simulation, a 100-year simulation was made starting with a uniform LAI of 1.0.

4.4. Response to a modified stomatal–atmospheric coupling

Numerous environmental factors can conceivably alter a hydrologic equilibrium. Climate change can alter VPD, which can in turn force an adjustment in stomatal regulation of water loss (Fig. 1). A change in climate can also bring about changes in soil temperatures that regulate microbial activity. These factors can combine in complex ways to alter site canopy density (Fig. 3). To isolate one factor alone the stomatal sensitivity to VPD was reduced by 50%. This has the effect of reducing the coupling between stomatal water regulation and atmospheric demand for water, which could occur naturally with a change

in species. In our context the change amounts to a higher stomatal conductance with no change in environmental conditions. This should produce higher photosynthetic rates and greater equilibrium canopy density at the expense of greater water losses, as long as water and nitrogen are not limiting. In particular, where nitrogen is limiting spatial patterns of canopy density should not change despite the higher stomatal conductance rates. Although transpiration rates are directly affected by factors limiting stomatal aperture, photosynthesis is ultimately limited by factors such as nutrition [8].

5. Results and discussion

5.1. Short-term gas exchange with a prescribed canopy

Fig. 7 shows relationships between measured and simulated turbulent flux for each of our 8 hillslopes. In

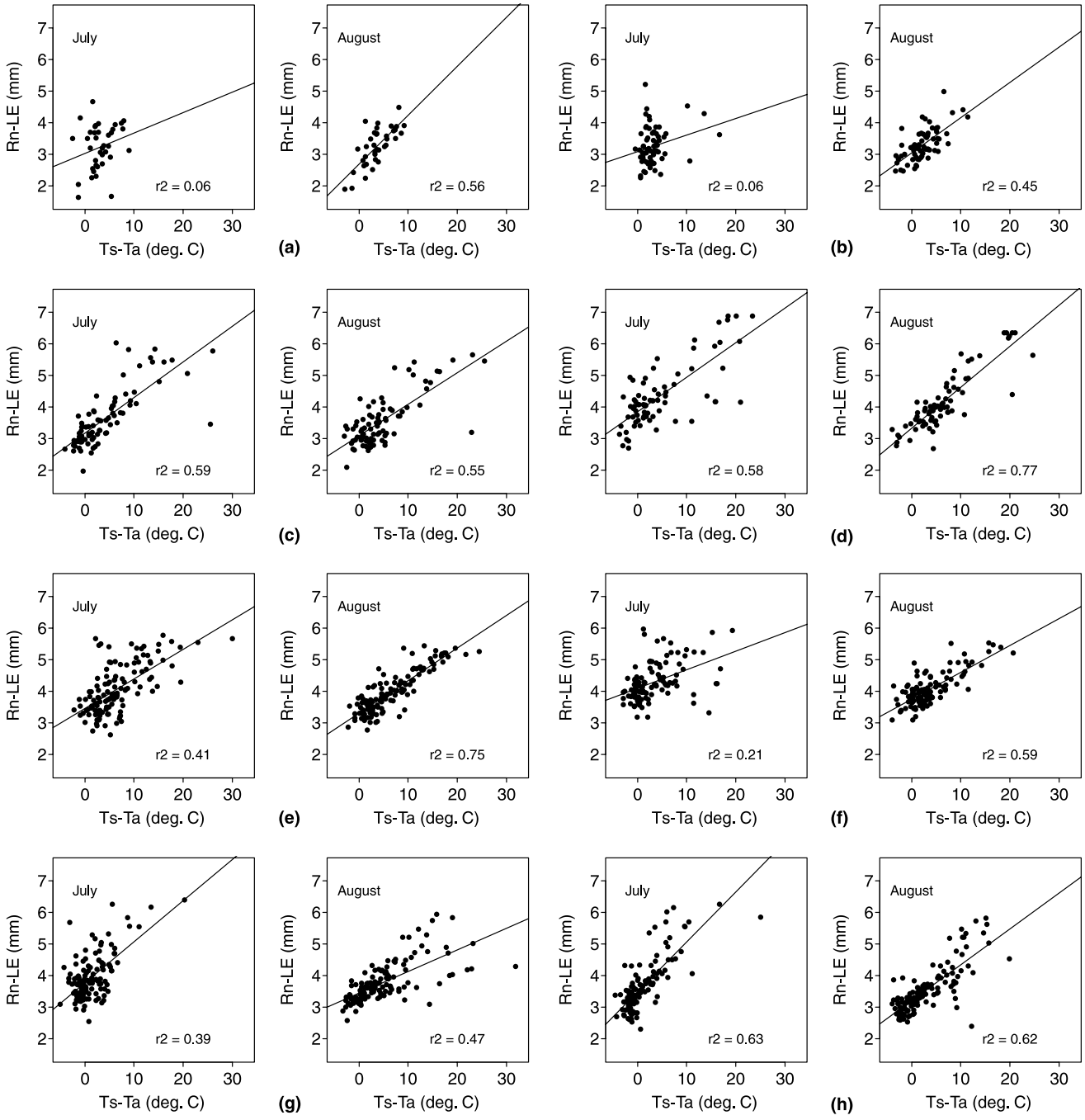

Fig. 7. Plots of simulated versus remotely sensed sensible heat flux, based on Eq. (13), for each of the 8 hillslopes (a–h) for both July 2 and August 6 scenes. Shown also are the linear regression line and accompanying variance explained.

general, the modeled energy balance explains a reasonable amount of variation in surface temperatures for all hillslopes on August 6. This is attributed to high wind speeds on this date [34] and hence greater canopy–atmosphere coupling. The model is a poor representation for hillslopes (a) and (b) on July 2. This is attributed to (1) lower wind speeds on this date and (2) the fact that these hillslopes face east and are at a lower elevation (Fig. 5), which further limits aerodynamic conductance. Improvements in prediction occur with west-facing hillslopes with steeper gradients and well-ventilated canopies, reflecting the fact that VPD is the primary control on stomatal aperture opening in this simulation. To test this hypothesis we disconnected the soil moisture control on stomatal conductance and observed no differences in latent heat fluxes. The responses of both transpiration and carbon assimilation are shown in Fig. 8 for a typical hillslope with a large elevation gradient. As expected trends in these outputs follow the trend in LAI with elevation. It is interesting to note that canopy flux responses with elevation can be divided into three segments. At low-slope positions canopy density is thinner and fluxes are lower. On initial inspection one might attribute this to canopy adjustment over time to soil water limitation. However, we also note that no moisture stress was simulated for the dates plotted, but that there was high VPD at the low elevation sites. Based on Figs. 1 and 2 we can suggest that transpiration rates reflect atmospheric drying power, and photosynthesis rates reflect a reduction in stomatal conductance rates. At mid-slope position the fluxes are relatively uniform with elevation, reflecting the nonlinearity of gas exchange responses to rates of water loss [17,30]. The flux rates then fall off at high elevation due to a low canopy density adjusted to low moisture content, as reflected by the predominance of drier sites at high elevation (see Fig. 8, TSI). This result does not imply that productivity rates are higher in these colder sites, but rather that the productivity relative to water consumed is higher here. Although this combined VPD–soil moisture explanation is not apparent from the fluxes shown in Fig. 8 it is confirmed when we look at WUE

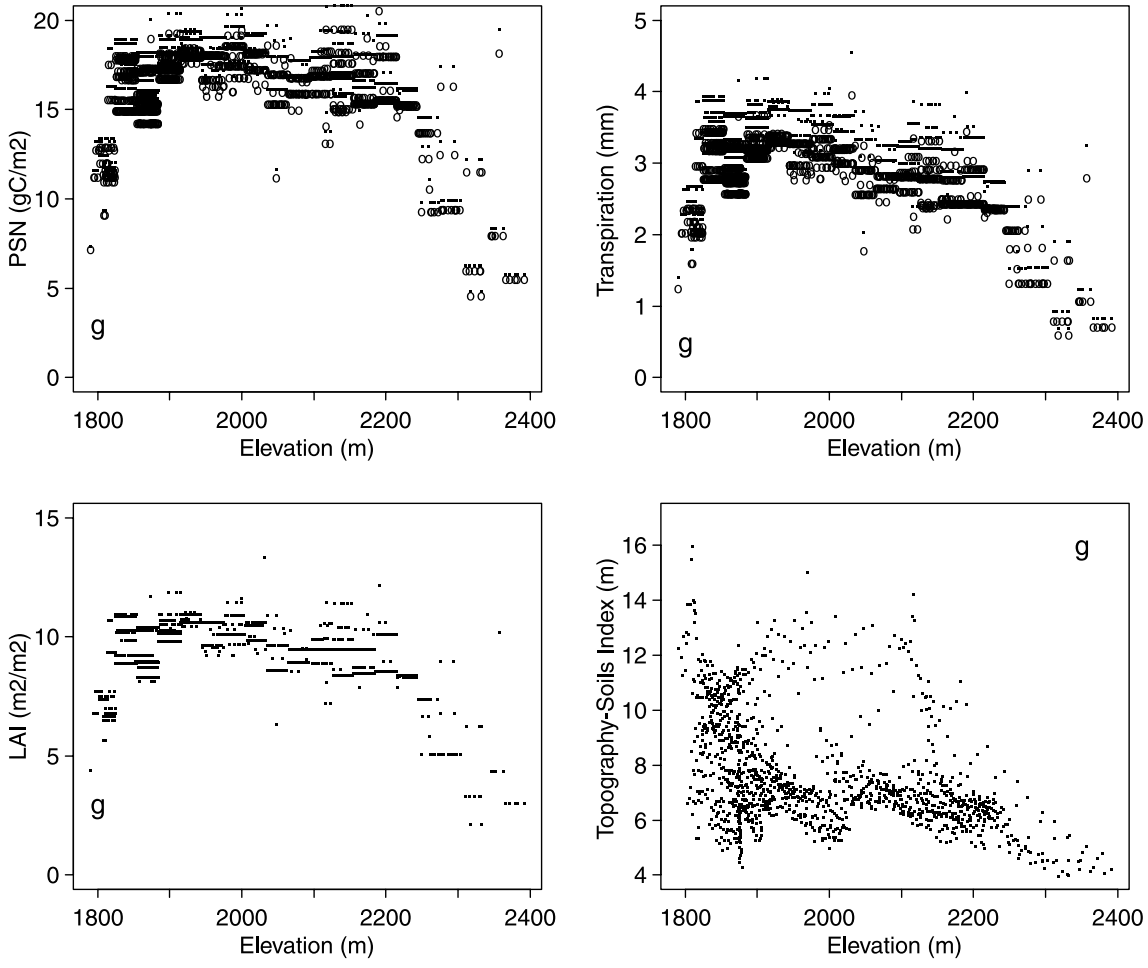

Fig. 8. Distributions of simulated fluxes (transpiration, net photosynthesis), remotely sensed LAI, and the TSI with respect to elevation, for hillslope *g*. For the flux plots, dots represent July 2 results and circles represent August 6 results.

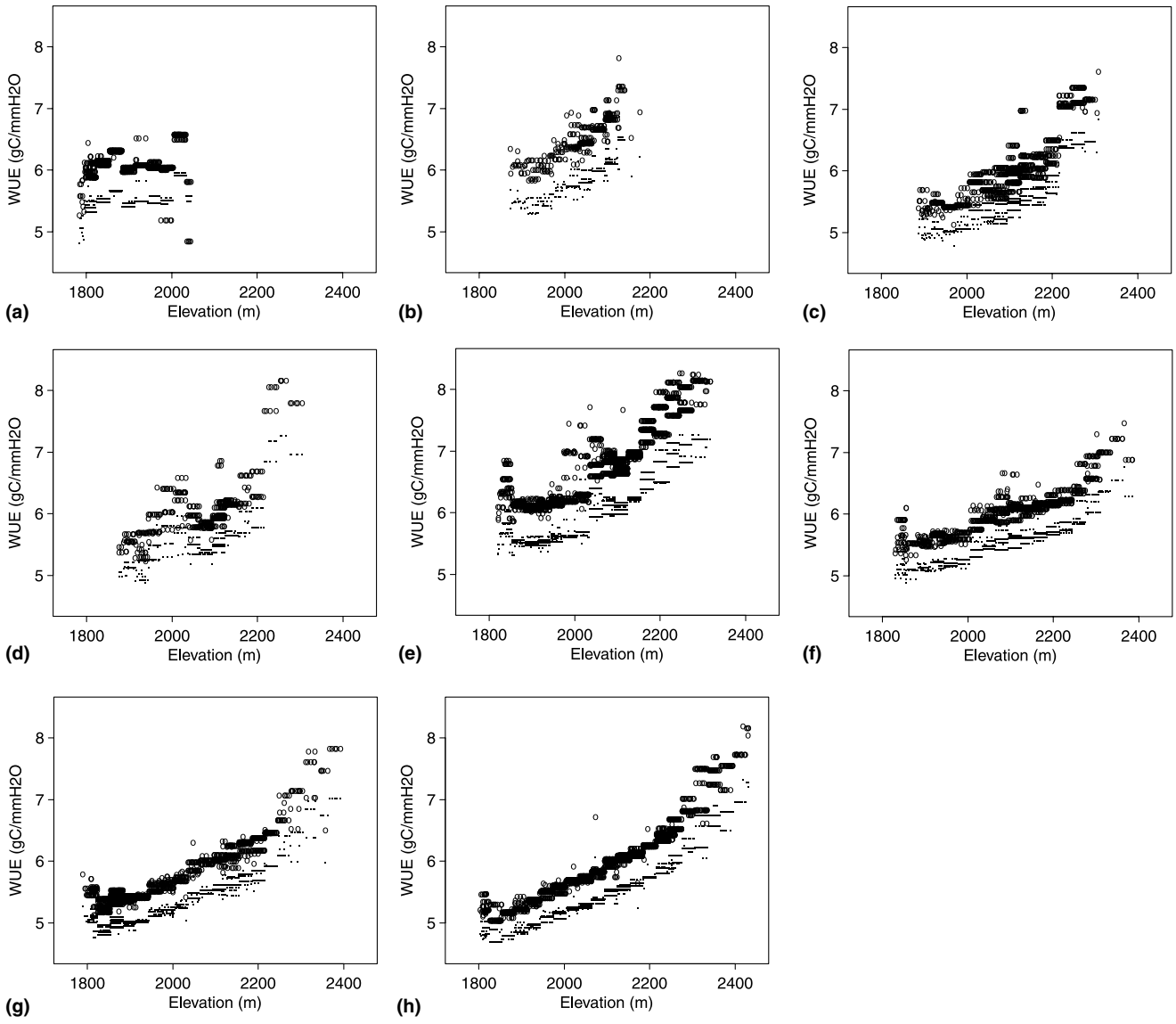

Fig. 9. Plots show WUE across elevation gradients within each of the 8 hillslopes used in this study. Dots represent July 2, while circles represent August 6 results.

Fig. 9). WUE is a measure of the water lost per unit of carbon fixed. WUE shows a clear upward trend with increasing elevation, reflecting lower maintenance respiration costs at cool high elevation sites, lower evaporative demand (and water loss) at high elevations, and higher CO_2 uptake by the higher stomatal conductance rates. It is important to note that WUE also responds to differences in VPD over time, as exhibited by higher WUE on the August 6 date, which had also had a higher VPD than July 2. These results support the existence of conservative water use by the forests of Onion Creek, which suggests that a strong water demand and supply control on the adjustment of canopy density over time. Stomatal regulation to atmospheric humidity has some adaptive advantages over a closure response to low water potentials, including the ability to continue to assimilate carbon for use in growing roots to seek out more water resources [24] and prevention of cell cavitation that produces permanent damage [43].

5.2. Canopy density adjustment

Fig. 10 shows predicted LAI compared with the remotely sensed LAI. Results derived from initially spatially uniform conditions in the litter and humus layers differ from those derived from spatially variable conditions. In general, LAI from the former initial conditions is more spatially uniform than the latter, suggesting that initial mineralization pools exert a lasting effect on canopy density. This is reflected both by the departures from the one-to-one line and in the variance explained. The spatially variable soil conditions result in a

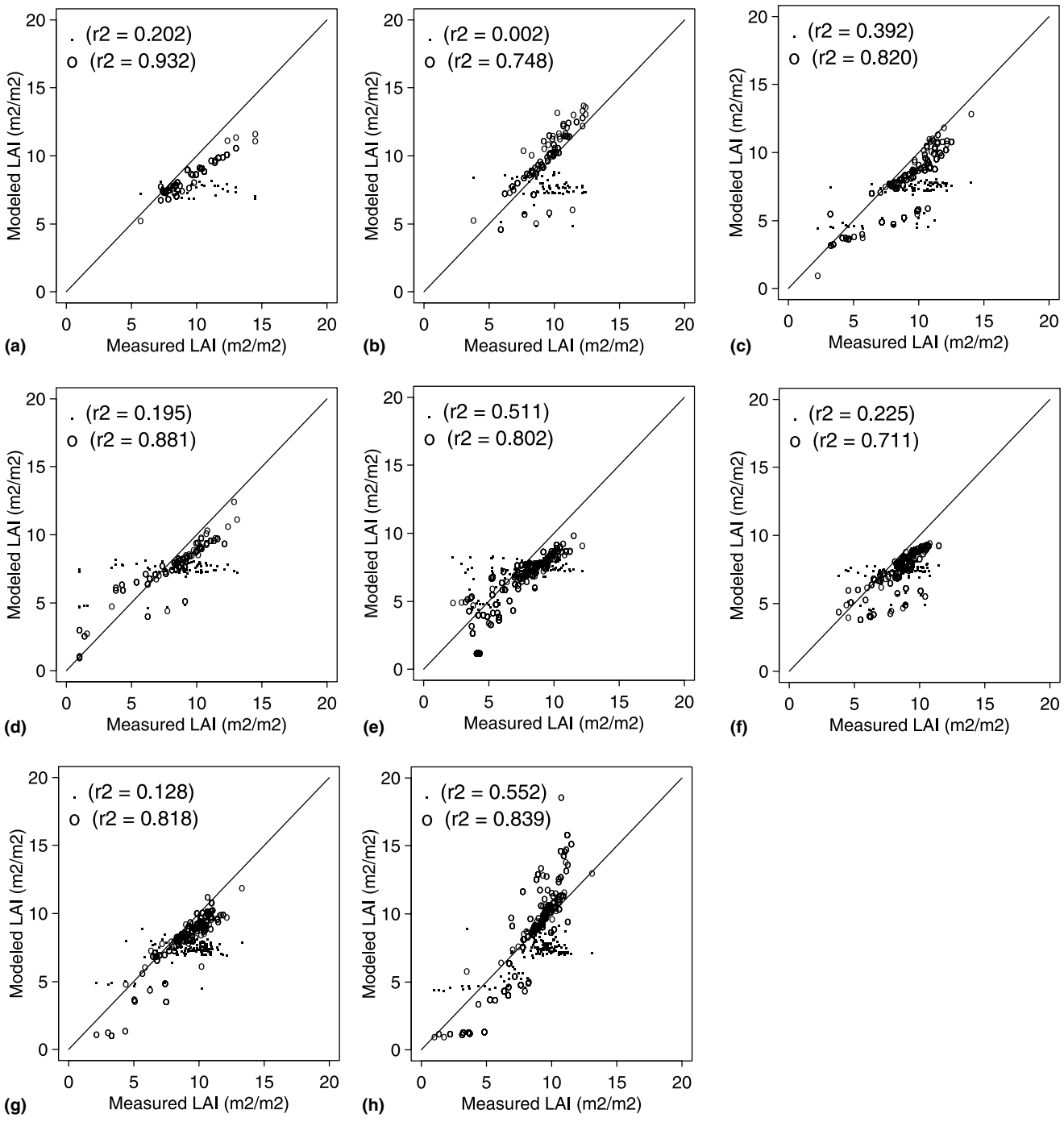

Fig. 10. Modeled LAI compared to remotely sensed measured LAI. Dots represent a simulation with soil carbon initialized as spatially uniform, and circles represent a simulation with initially spatially variable soil carbon. All simulated LAI values are taken from year 50, which is when the catchment average modeled and measured LAIs are approximately equal. Shown also are 1:1 lines and associated LAI variance explained by the spatially variable soil carbon simulation.

considerably improved prediction of LAI by providing a more realistic response in sites not experiencing water stress. This soil memory effect is illustrated in Fig. 11, which shows that an initial spatial pattern is partially preserved as the canopy develops. By initializing the model with spatially uniform soil carbon an overly simple equilibrium canopy density emerges. It conforms to soil water and VPD controls as predicted, but it lacks the variability associated with nutrient dynamics. As a result, the overly aggregated nutrient dynamics fail to reproduce spatial patterns of LAI. Alternatively, the LAI reproduced by incorporating a spatially variable initial soil carbon corresponds well with the hypothetical

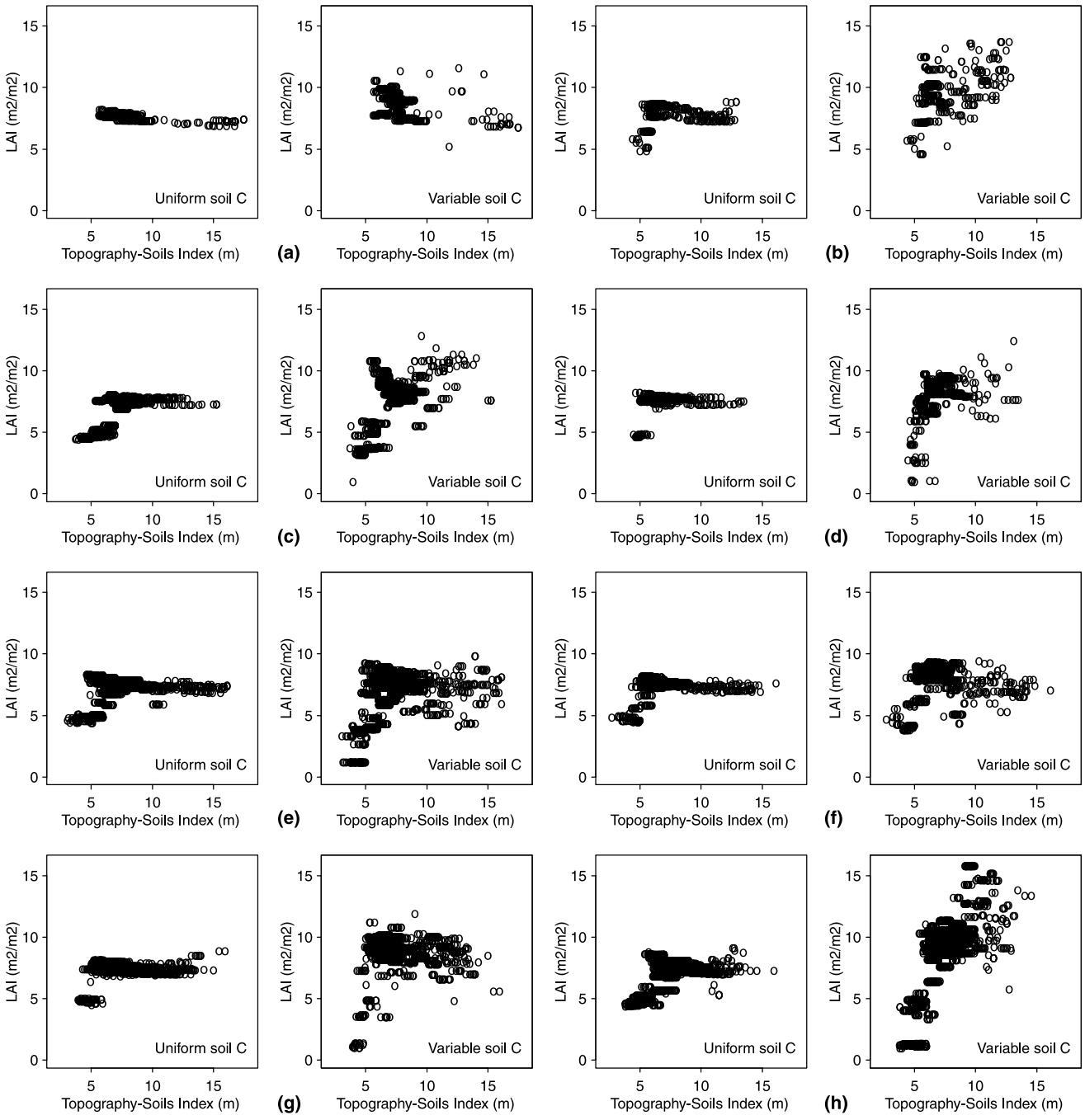

Fig. 11. Plots of simulated LAI along catenary sequences represented by the TSI, for both uniform and spatially variable soil carbon.

relation between canopy density and catenary position (compare to Fig. 3).

5.3. Adjustment of canopy density with a reduced stomatal–VPD response

At low to medium LAI values there is no apparent increase in canopy density associated with reduced stomatal sensitivity to VPD (Fig. 12). Instead, LAI at these levels appears to acclimate to an alternative limitation besides VPD. This can be partially explained by soil water limitation at the lowest LAI values. At higher LAI values there is a dramatic increase in canopy density on some hillslopes as the stomatal regulation is reduced. This can be attributed to differences in nitrogen limitation between hillslopes. Hillslopes a, b, and e are cooler east- to southeast facing (see Fig. 5), whereas the other hillslopes are warmer southwest to west facing. The warmer conditions promote higher N mineralization rates that are better able to keep pace with the in-

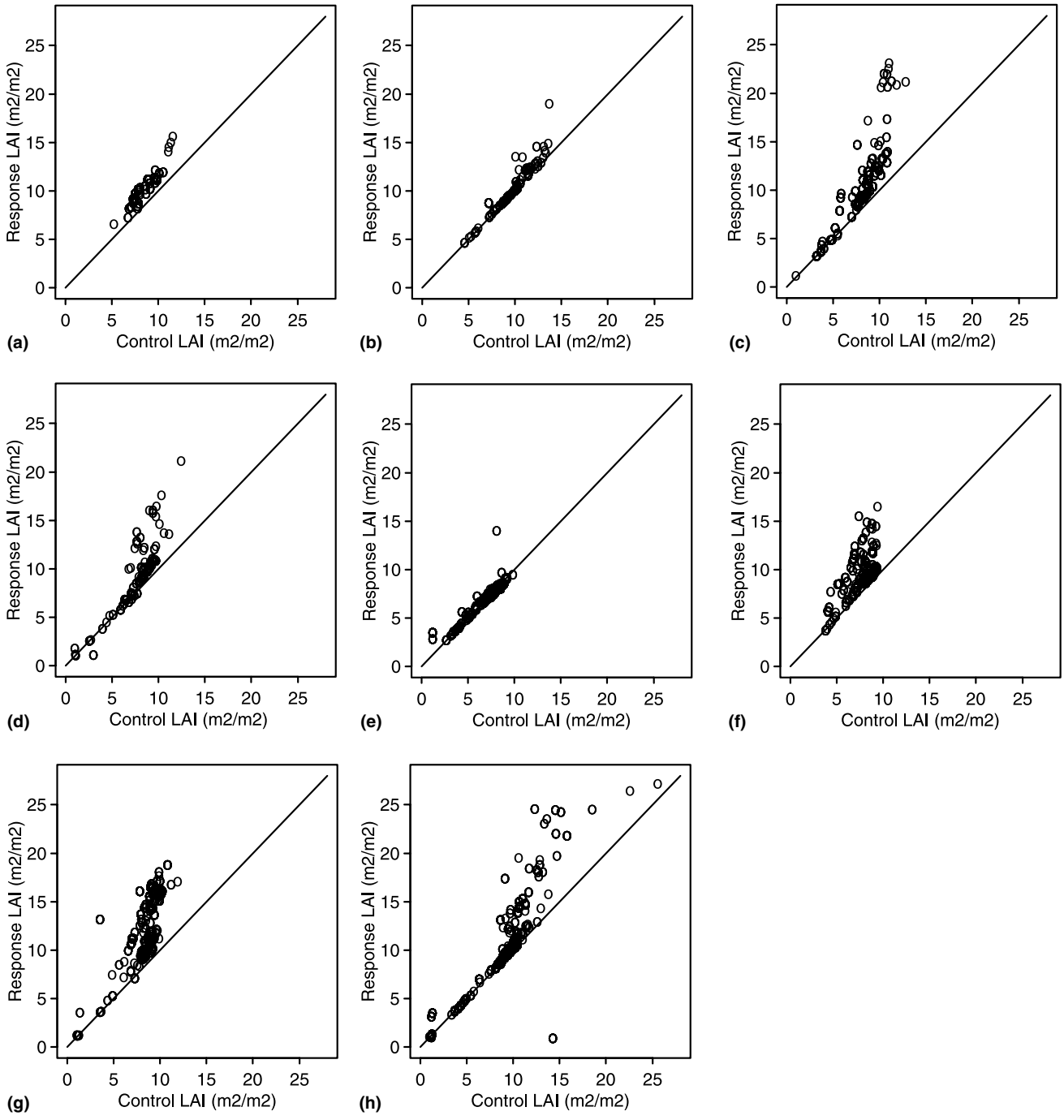

Fig. 12. Plots of simulated LAI with reduced stomatal–VPD coupling (Response LAI) versus simulated LAI under normal coupling (Control LAI), for each of the 8 hillslopes in this study.

creased CO_2 uptake. Similar acclimation occurs with increased ambient levels of CO_2 because of N limitations. Unless N availability can keep up with the carbon fixation costs of higher CO_2 little change in carbon assimilation is observed [18].

Fig. 13 shows the growing season trends in catchment average responses of Bowen ratio, pre-dawn leaf water potential and WUE to reduced sensitivity of stomatal conductance to VPD. The increased stomatal apertures resulting from the reduced physiological response to VPD results in greater water losses, as reflected by lower Bowen ratios and lower leaf water potentials. The Bowen ratio is most affected at times when soil moisture levels are high, such as around July 2. By August 6 latent heat fluxes have adjusted downward in response to drying soil to produce a response Bowen ratio comparable to that of the control simulation. This adjustment is attributed to stomatal closure due to leaf water

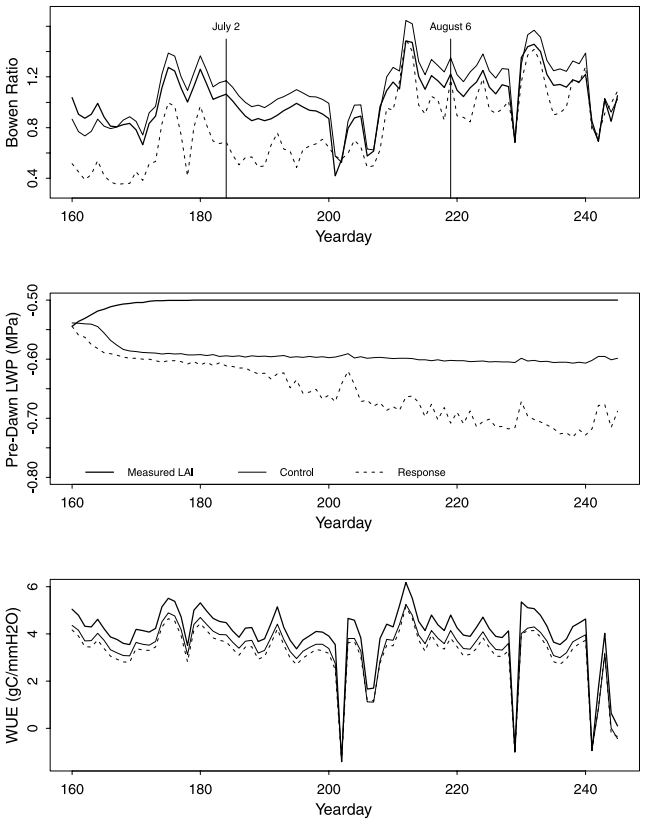

Fig. 13. Time series plots of Bowen Ratio, pre-dawn leaf water potential, and WUE, using remotely sensed (Measured) LAI and normal stomatal–VPD control, LAI simulated with normal stomatal–VPD coupling (Control), and LAI simulated with reduced stomatal–VPD control. Vertical lines indicate dates of thermal remote sensing scenes, and are included to highlight the increase in Bowen Ratio (or lower relative amount of evaporation) on August 6 versus July 2.

potential, which falls throughout the period shown. However, it is interesting to note that WUE decreases only slightly in response to the reduced stomatal sensitivity, a result that is consistent with the increased growth in canopy density shown in many of the hillslopes in Fig. 12. The slight decrease in WUE is caused by nitrogen limitation in some areas where the pace of canopy development outstrips the rate of increase in nitrogen available to the vegetation. These results support the notion of an average canopy density that is adjusted to the physiological controls on water use such that damaging water stress is avoided [43]. However, in specific sites nutrient limitations are critical for determining actual canopy density, regardless of stomatal regulation of water potentials.

6. Conclusions

We began with the hypothesis that canopy density in coniferous forests can be explained in terms of a modified hydrologic equilibrium that incorporates soil moisture, atmospheric humidity (or VPD), and nitrogen availability. With respect to spatial patterns of canopy density it was argued that soil moisture and atmospheric conditions, the main elements of ecological optimality [7] and hydrologic equilibrium [31] can explain catchment-wide trends, but not detailed spatial patterns of canopy density. Simulated LAI using an aspatial initialization of soil carbon and nitrogen shows a soil memory effect, in which initial soil carbon and nitrogen establish a persistent turnover cycle. Actual patterns of LAI can be predicted when some spatial knowledge of the soil pools can be obtained. It should reflect historical land cover and land use changes, including fire, forest harvesting, and vegetation succession. Here we had a relatively simple system with an old-growth forest, which was assumed to be in equilibrium with the surface and subsurface nutrient pools. In disturbed catchments the long-term canopy–atmosphere gas exchanges may be difficult to simulate without a detailed knowledge of soil development. The existence of a hydrologic equilibrium in Onion Creek is partly supported by the simulations presented in this paper. It is reflected in the coupling of carbon and water through stomatal regulation of water use in the short term, and the allocation of carbon within the plant over the long term. However, it seems unreasonable to make prediction of carbon–water relations over extended periods of time without considering nitrogen limitations, which are inherent in most natural ecosystems.

The simulations here indicate that, for long-term distributed catchment modeling, there should be an increased focus on understanding site history (disturbance, land use, etc.). There is a persistence or memory effect in the soil, which cannot be discounted in models of long-term adjustment of canopy gas exchange. The soil carbon and nitrogen pools reflect long-term land use and land use changes, vegetation succession patterns, climate, and topography. Water availability or soil recharge rate is a critical term for explaining the distribution of vegetation–atmospheric interactions in water-limited conditions. However, the existence of a hydrologic equilibrium or ecological optimality is complicated by a need to consider the carbon cost and nutrient limitation on carbon fixation. The removal or reduction of one gas exchange rate-limiting factor, such as VPD, may simply reveal another limiting factor, such as available water or nitrogen. While such limitations may average out over a catchment or larger area, specific locations within a catchment may be affected by different forms of canopy growth limitations, which can provide important feedbacks on vegetation water use along topography-driven hydrologic flow paths.

There has been a resurgence of interest in hydrologic equilibrium with a specific focus on revisiting issues related to Eagleson's theories [35]. These approaches at-

tempt to incorporate biological responses into aspatial analytical water balance equations. The present study approaches this same problem using process-based models that adjust spatial patterns of carbon and water over time to climate forcing. This directly incorporates carbon cost in searching for equilibrium soil–topography–vegetation relations. It would be interesting to compare these analytical and simulation approaches, since key differences between them occur in carbon and nitrogen cycling feedbacks working in concert with stomatal regulation of canopy gas exchange. In turn it would be useful to compare model results to field investigations into forest stand level water balance, such as sap flux [33].

7. Acknowledgements

Funding for this research was provided from NASA Land Surface Hydrology Program grant #NAG5-8554. The author also acknowledges funding from McIntire-Stennis. Data for Onion Creek was furnished by Rama Nemani and Lars Pierce. An anonymous reviewer and Praveen Kumar are thanked for their feedback on the manuscript.

References

[1] Arris LL, Eagleson PS. A water use model for locating the boreal/deciduous forest ecotone in eastern North America. Water Resour Res 1994;30(1):1–9.
[2] Band LE, Patterson P, Nemani R, Running SW. Forest ecosystem processes at the watershed scale: incorporating hillslope hydrology. Agric For Meteorol 1993;63:93–126.
[3] Beven K. Runoff production and flood frequency in catchments of order *n*: an alternative approach. In: Gupta VK, editor. Scale problems in hydrology. Hingham, MA: D. Reidel; 1986. p. 107–31.
[4] Beven KJ, Kirkby MJ. A physically based, variable contributing area model of basin hydrology. Hydrol Sci Bull 1979;1:43–69.
[5] Calder IR. Water use by forests, limits and controls. Tree Physiol 1998;18:625–31.
[6] Carlson TN, Capehart WJ, Gillies RR. A new look at the simplified method for remote sensing of daily evapotranspiration. Remote Sensing Environ 1995;54:161–7.
[7] Eagleson PS. Ecological optimality in water-limited natural soil–vegetation systems 1. Theory and hypothesis. Water Resour Res 1982;18(2):325–40.
[8] Farquhar GD, Sharkey TD. Stomatal conductance and photosynthesis. Ann Rev Plant Physiol 1982;33:317–45.
[9] Field C, Merino J, Mooney HA. Compromises between water-use efficiency and nitrogen-use efficiency in five species of California evergreens. Oecologia 1983;60:384–9.
[10] Gardner WR. Some steady-state solutions of the unsaturated moisture flow equation with application to evaporation from a water table. Soil Sci 1958;85:228–32.
[11] Giardina CP, Ryan MF. Evidence that decomposition rates of organic carbon in mineral soil do not vary with temperature. Nature 2000;404:858–61.
[12] Goldstein AH, Hultman NE, Fracheboud JM, Bauer MR, Panek JA, Xu M, Qi Y, Geunther AB, Baugh W. Effects of climate variability on the carbon dioxide, water, and sensible heat fluxes above a ponderosa pine plantation in the Sierra Nevada (CA). Agric For Meteorol 2000;101:113–29.
[13] Grier CC, Running SW. Leaf area of mature northwestern coniferous forests: relation to site water balance. Ecology 1977;58:893–9.
[14] Harrison KG, Post WM, Richter DD. Soil carbon turnover in a recovering temperate forest. Global Biogeochem Cycles 1995;9(4):449–54.
[15] Jackson RD, Reginato RJ, Idso SB. Wheat canopy temperature: a practical tool for evaluating water requirements. Water Resour Res 1977;13:651–6.
[16] Jarvis PG. The interpretation of the variations in leaf water potential and stomatal conductance found in canopies in the field. Philos Trans R Soc London, Ser B 1976;273:593–610.
[17] Jarvis PG. Stomatal response to water stress in conifers. In: Turner NC, Kramer PJ, editors. Adaptation of plants to water and high temperature stress. New York: Wiley; 1980. p. 105–22.
[18] Jarvis PG. Global change and plant water relations. In: Borghetti M, Grace J, Raschi A, editors. Water transport in plants under climatic stress. Cambridge: Cambridge University Press; 1993. p. 1–13.
[19] Keyes MR, Grier CC. Above- and below-ground net production in 40-year-old Douglas-fir stands on low and high productivity sites. Can J For Res 1981;11:599–605.
[20] Kirschbaum MUF. The temperature dependence of soil organic matter decomposition, and the effect of global warming on soil organic C storage. Soil Biol Biochem 1995;27:753–60.
[21] Kramer PJ, Boyer JS. Water relations of plants and soils. San Diego, CA: Academic Press; 1995.
[22] Larcher W. Physiological plant ecology. 3rd ed. Berlin: Springer; 1995.
[23] Lohammar T, Larsson S, Linder S, Falk SO. FAST-simulation models of gaseous exchange in Scots pine. In: Persson T, editor. Structure and function of Northern Coniferous forests – an ecosystem study. . Ecol Bull 1980;32:505–23.
[24] Ludlow MM. Adaptive significance of stomatal responses to water stress. In: Turner NC, Kramer PJ, editors. Adaptation of plants to water and high temperature stress. New York: Wiley; 1980. p. 123–38.
[25] MacDonald LH. Forest harvest, snowmelt and streamflow in the central Sierra Nevada. Forest Hydrology and Watershed Management. In: Proceedings of the Vancouver Symposium; August, 1987. p. 273–83.
[26] MacDonald LH. Persistence of soil moisture changes resulting from artificially extended snowmelt. In: Proceedings of the Annual Western Snow Conference, 54th Annual Meeting, Phoenix, Arizona. Fort Collins, CO: Colorado State University Press; April 15–17, 1985. p. 146–9.
[27] Mackay DS, Band LE. Forest ecosystem processes at the watershed scale: dynamic coupling of distributed hydrology and canopy growth. Hydrol Process 1997;11:1197–217.
[28] Maier-Maercker U. Dynamics of change in stomatal response and water status of *Picea abies* during a persistent drought period: a contribution to the traditional view of plant water relations. Tree Physiol 1998;18:211–22.
[29] Monteith JL. Evaporation and environment. In: Proceedings of the 19th Symposium of the Society for Experimental Biology. New York: Cambridge University Press; 1965. p. 205–33.
[30] Monteith JL. A reinterpretation of stomal response to humidity. Plant Cell Environ 1995;18:357–64.
[31] Nemani RR, Running SW. Testing a theoretical climate–soil–leaf area hydrological equilibrium of forests using satellite data and ecosystem simulation. Agric For Meteorol 1989;44:245–60.

[32] Nieuenhuis GJA, Schmidt EA, Tunnissen HAM. Estimation of regional evapotranspiration of arable crops from thermal infrared images. Int J Remote Sensing 1985;6:1319–34.
[33] Oren R, Ewers BE, Todd P, Phillips N, Katul G. Water balance delineates the soil layer in which moisture affects canopy conductance. Ecol Appl 1998;8(4):990–1002.
[34] Pierce LL, Congalton RG. A methodology for mapping forest latent heat flux densities using remote sensing. Remote Sensing Environ 1988;24:405–18.
[35] Rodriguez-Iturbe I. Ecohydrology: a hydrologic perspective of climate–soil–vegetation dynamics. Water Resour Res 2000;36(1):3–9.
[36] Running SW, Coughlan JC. A general model of forest ecosystem processes for regional applications I. Hydrologic balance, carbon gas exchange and primary production processes. Ecol Modelling 1988;42:125–54.
[37] Running SW, Gower ST. FOREST-BGC, a general model of forest ecosystem processes for regional applications II. Dynamic carbon allocation and nitrogen budgets. Tree Physiol 1991;9:147–60.
[38] Running SW, Hunt Jr ER. Generalization of a forest ecosystem process model for other biomes, BIOME-BGC, and an application for global scale models. In: Ehleringer JR, Field CB, editors. Scaling physiological processes: leaf to globe. San Diego, CA: Academic Press; 1993. p. 141–58.
[39] Running SW, Nemani R, Hungerford RD. Extrapolation of synoptic meteorological data in mountainous terrain, and its use for simulating forest evapotranspiration and photosynthesis. Can J For Res 1987;17:472–83.
[40] Schlesinger WH. Biogeochemistry: an analysis of global change. 2nd ed. San Diego, CA: Academic Press; 1997.
[41] Seguin B, Itier B. Using midday surface temperature to estimate daily evaporation from satellite thermal IR data. Int J Remote Sensing 1983;4:371–83.
[42] Sivapalan M, Beven K, Wood EF. On hydrologic similarity 2. A scaled model of storm runoff production. Water Resour Res 1987;23(12):2266–78.
[43] Tyree MT, Ewers FW. The hydraulic architecture of trees and other woody plants. New Phytol 1991;119:345–60.
[44] Van Genuchten MTh. A closed-form equation for predicting the hydraulic conductivity of unsaturated soils. Soil Sci Soc Am J 1980;44:892–8.
[45] Vertessy RA, Hatton TJ, Benyon RG, Dawes WR. Long-term growth and water balance predictions for a mountain ash (*Eucalyptus regnans*) forest catchment subject to clear-felling and regeneration. Tree Physiol 1996;16:221–32.
[46] Waring RH, Running SW. Forest ecosystems: analysis at multiple scales. San Diego, CA: Academic Press; 1998.
[47] Waring RH, Schlesinger WH. Forest ecosystems: concepts and management. San Diego, CA: Academic Press; 1985.
[48] Whitehead D. Regulation of stomatal conductance and transpiration in forest canopies. Tree Physiol 1998;18:633–44.
[49] Wigmosta MS, Vail LW, Lettenmaier DP. A distributed hydrology–vegetation model for complex terrain. Water Resour Res 1994;30(6):1665–79.
[50] Woodward FI. Climate and plant distribution. Cambridge: Cambridge University Press; 1987.